Chapter 1

Introduction

1.1 Liquid Crystals

Liquid crystals are intermediate states of matter, which exhibit properties of both liquids and crystals [1]. In liquids, the molecules are mobile and have no orientational or positional order. In crystals, the molecules have no mobility and are located in regular repeating positions. This leads to long range order in both position and orientation. In liquid crystals, the molecules exhibit intermediate properties; a combination of both order and mobility (Figure 1.1). For this reason, they are also called intermediate phases or mesophases. The molecules which exhibit such intermediate phases are referred to as **mesogens**.

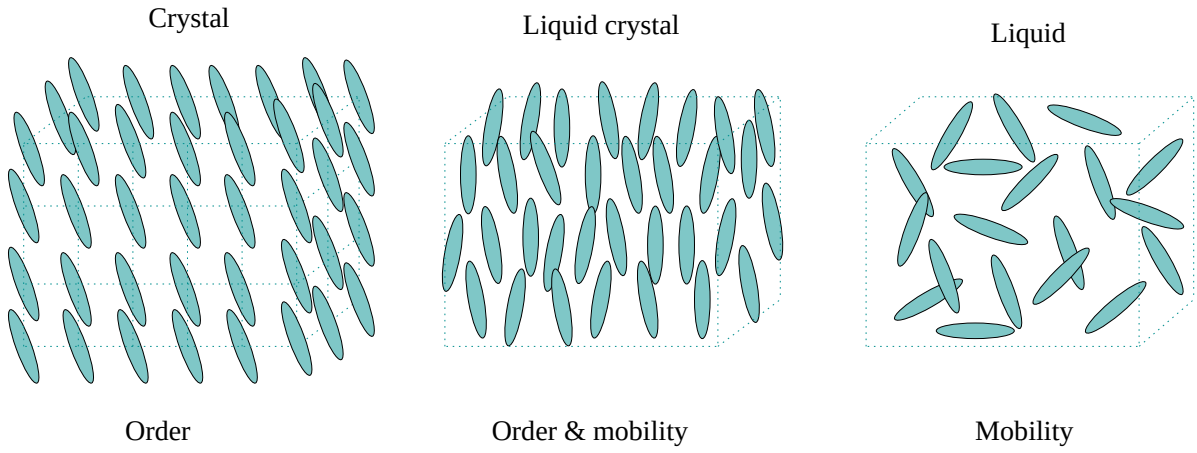

Figure 1.1: A schematic representation of basic structural differences among crystal, liquid crystal and liquid.

Liquid crystals (LCs) can be broadly classified into two categories: (a) **Thermotropic**, where the mesophase formation is temperature dependent [2]. (b) **Lyotropic**, where the mesophase for-

mation is solvent and concentration dependent [3]. The thermotropic LCs are of interest from the standpoint of both basic research as well as applications in electro-optic displays, temperature and pressure sensors. On the other hand, lyotropic LCs are of great interest biologically and appear to play an important role in living systems.

In the following subsections, we briefly describe the main features of commonly occurring mesophases such as nematic, cholesteric and smectic phases.

1.1.1 Nematic Phase

The nematic phase is the least ordered mesophase in which the molecules possess only long range orientational order but no positional order. The word "nematic" comes from the Greek word "nematos" meaning thread. It refers to certain thread like defects which are commonly observed under the optical microscope. In this phase, the molecules are spontaneously oriented with their long axes approximately parallel to a preferred direction. The preferred direction of orientation of the molecules is represented by a unit vector **n**, and is called the director. This is shown as an arrow in Figure 1.2.

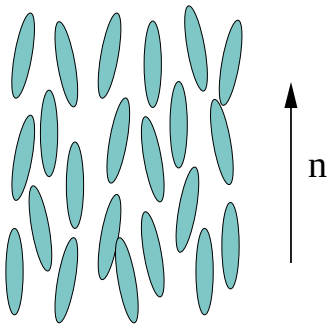

Figure 1.2: Arrangement of molecules in nematic liquid crystalline phase.

1.1.2 Cholesteric Phase

The cholesteric (or chiral nematic) phase is exhibited by molecules which are either chiral[1] in nature or doped in small quantities with chiral molecules. The structure of a cholesteric liquid crystal is shown in Figure 1.3. It consists of molecules in a statistically parallel arrangement of the director **n** just like the nematic phase. However, the asymmetry of the constituent molecules

[1] An object or molecule that is not superimposable on its mirror image is known as chiral.

causes a slight and gradual spontaneous rotation of the director. The director describes a helix with a specific temperature dependent pitch.

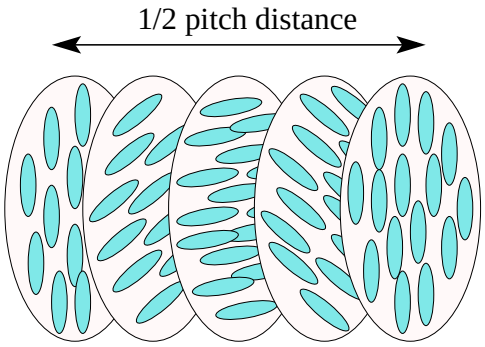

Figure 1.3: Schematic representation of cholesteric liquid crystalline phase.

1.1.3 Smectic Phase

In smectic (from Greek word "smectos" meaning soap) phase, the molecules possess positional order in addition to the orientational order. The molecules are arranged in layers with a well-defined layer spacing or periodicity. The smectic phases, being more ordered than nematics, generally occur at temperatures below the nematic phase. There are several types of smectic mesophases, characterized by a variety of molecular arrangements within the layers. The most common are the smectic A and smectic C phases (Figure 1.4). In smectic A phase, the molecules form layers with their long axes parallel to the layer normal. The smectic C phase has the same layer structure as that of the smectic A, but the molecules are tilted with respect to the layer normal. In both the phases, there is no positional order between molecules within the layers.

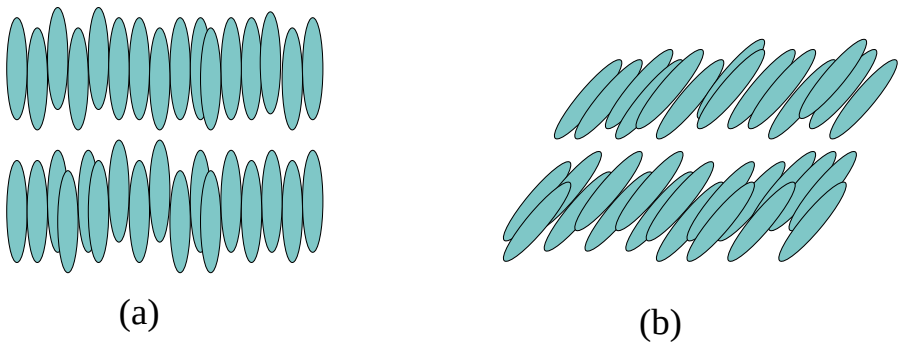

Figure 1.4: Arrangement of molecules in smectic liquid crystalline phase. (a) Smectic A. (b) Smectic C.

The fundamental requirement for a material to exhibit a LC phase is the shape anisotropy of the constituent molecules. On the basis of the shape of mesogenic molecules, LCs can be further classified into three main structural groups: **Calamitic** (the constituent molecules are rod-like), **Discotic** (the constituent molecules are disk-like), and **Bent-shape** (the constituent molecules are banana-like).

1.2 Discotic Mesophase

The self organization of disk-shaped molecules leads to the formation of discotic mesophases [4]. The molecules that exhibit discotic mesophase are called discotic mesogens. In this section, we briefly describe different mesophases exhibited by discotic molecules.

1.2.1 Discotic Nematic Phase

In the discotic nematic phase, the molecules stay more or less in parallel position having only orientational order but no long range positional order. Here, the disk-like molecules possess full translational and rotational freedom around their short axes, whereas their long axes (spanning the plane of the discotic mesogen) orient, on average, parallel to a general plane. Like cholesteric phase, chiral discotic nematic mesophases also exist. This mesophase occurs in mixtures of discotic nematic and non-mesogenic chiral dopants, as well as in pure chiral discotic molecules. In addition, a nematic columnar phase can exist which is characterized by a columnar stacking of the discotic molecules. However, these columns do not form two-dimensional lattice structures. They display a positional short-range order and an orientational long-range order. The different nematic phases exhibited by discotic molecules are shown in Figure 1.5.

1.2.2 Discotic Columnar Phase

In discotic columnar phase, the molecules assemble themselves one on top of the other in columns packed parallel on a two-dimensional lattice. Depending on the order in the molecular stacking in the columns and the two-dimensional lattice symmetry of the column packing, the columnar mesophases may be classified into several classes; hexagonal, rectangular, oblique and lamellar. Columnar hexagonal phase is characterized by a hexagonal packing of the molecular columns.

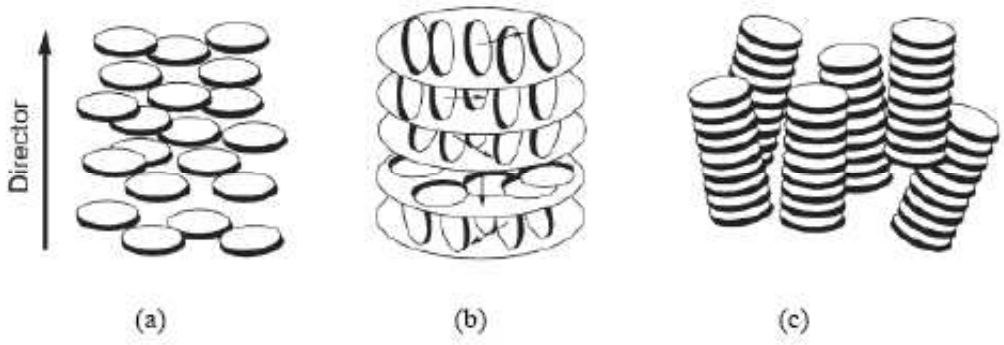

Figure 1.5: Schematic representation of discotic liquid crystalline phases; (a) nematic, (b) chiral nematic and (c) nematic columnar.

The columnar rectangular mesophase consists of the stacking of the aromatic cores of molecules in columns surrounded by the disordered aliphatic chains and packed in a rectangular fashion. In columnar oblique mesophase, the columns are arranged with an oblique unit cell. In columnar lamellar mesophase the constituent molecules stack into columns which are further arranged in a layered structure. We have represented these phases pictorially in Figure 1.6.

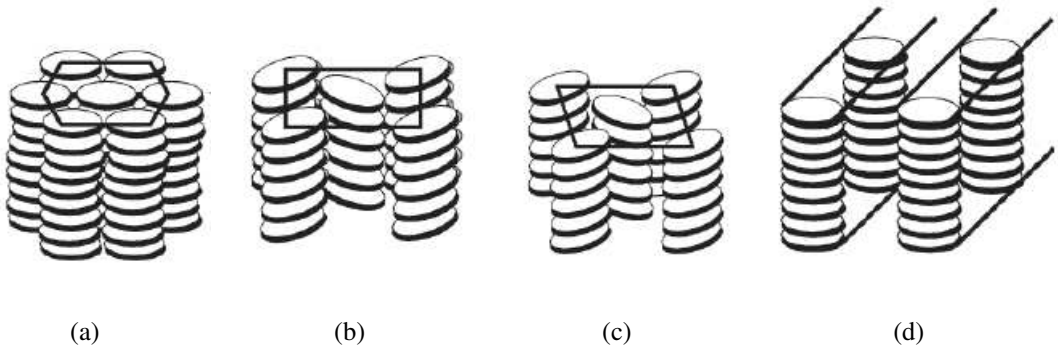

Figure 1.6: Schematic representation of different columnar phases exhibited by discotic mesogens; (a) hexagonal, (b) rectangular, (c) oblique and (d) lamellar.

1.3 Discotic Mesogens

In 1977, it was established that benzene hexa-n-alkanoates form a new class of liquid crystals [5] in which molecules are stacked one on the top of other in columns that constitute a hexagonal arrangement (Figure 1.7). This opened a whole new field of fascinating liquid crystal research.

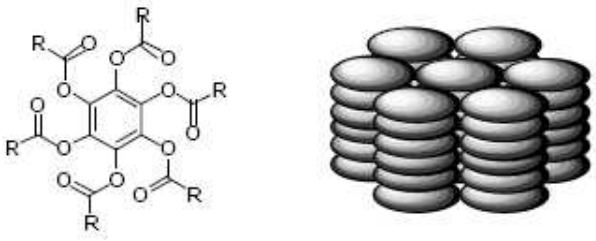

Figure 1.7: Structure of benzene-hexa-n-alkanoates and their columnar arrangement.

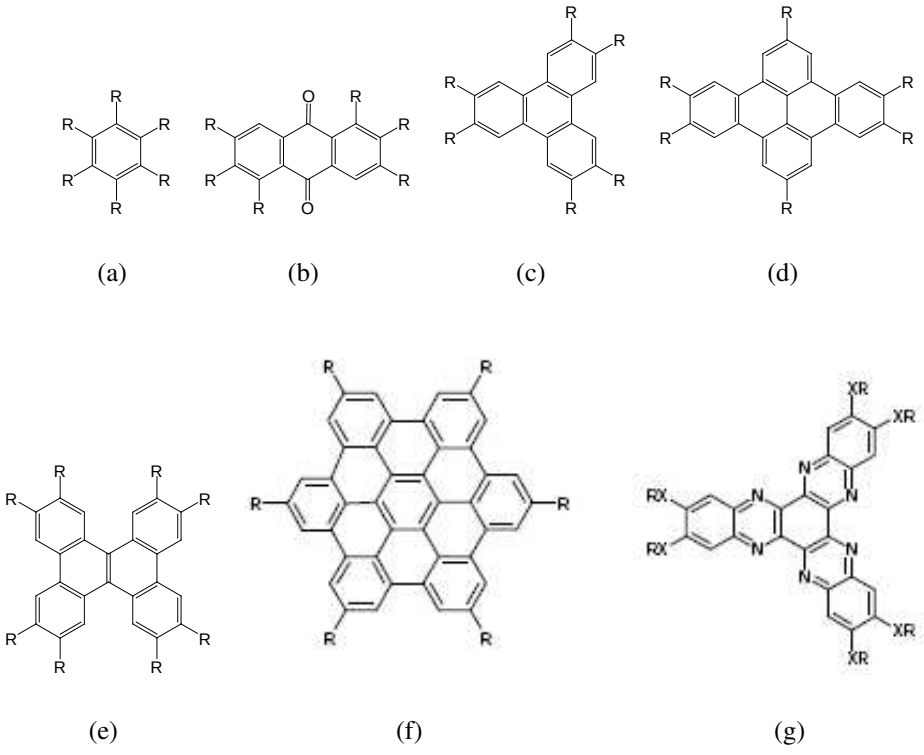

Figure 1.8: A general molecular architecture of discotic mesogens with various cores. R=alkyl chain.

Discotic mesogens generally consist of flat, rigid aromatic cores surrounded by flexible alkyl chains. A general molecular architecture for discotic mesogens is shown in Figure 1.8. Discotic mesogens are of interest for their intriguing supramolecular architectures. The intense π-π interaction of polyaromatic cores leads to columnar structure. The core-core separation in a columnar mesophase is usually of the order of 0.35 nm so that there is considerable overlap of π orbitals. As flexible long aliphatic chains surround the core, the intercolumnar distance is usually 2-4 nm, depending on the lateral chain length. Therefore, interactions between the neighboring molecules within the same column would be much stronger than interactions between neighboring columns. Consequently, charge migration in these materials is expected to be quasi-one dimensional [4].

Discotic mesogens are known as a new generation of organic semiconductors because of their unique molecular electronic properties. Some of the known examples of successfully operating devices based on discotic semiconductors are field-effect transistor, light-emitting diode and photovoltaic solar cell [6]. In addition, there have been continuous efforts for using these materials in gas sensors, liquid crystal displays and memory devices [7].

1.4 Amphiphiles

Amphiphiles are molecules which consist of two parts; one part is **hydrophilic** and the other part is **hydrophobic**. The classical example is a long-chain fatty acid (or alcohol) where the -COOH (or -OH) is the polar hydrophilic part and the aliphatic chain is the hydrophobic part. When such molecules are put on water surface, the hydrophilic part of the molecules easily form hydrogen bonds with water molecules and hence get anchored to the water surface. The hydrophobic part of the molecules do not form hydrogen bonds with water and hence favors to stay away from the water surface. Consequently, a monolayer of such molecules is formed at the air-water (A-W) interface (Figure 1.9).

A wide variety of amphiphiles (amphiphilic molecules) are known to form stable monolayer at A-W interface [8]. The degree of stability of an amphiphile at A-W interface is decided by its hydrophilic-hydrophobic balance. The polar groups may be - CN, -$CONH_2$, -C_6H_4OH, -SO_3^-, -NH_3^+ and -$C_6H_4SO_4^-$. The length of the hydrocarbon chains required varies with the polarity

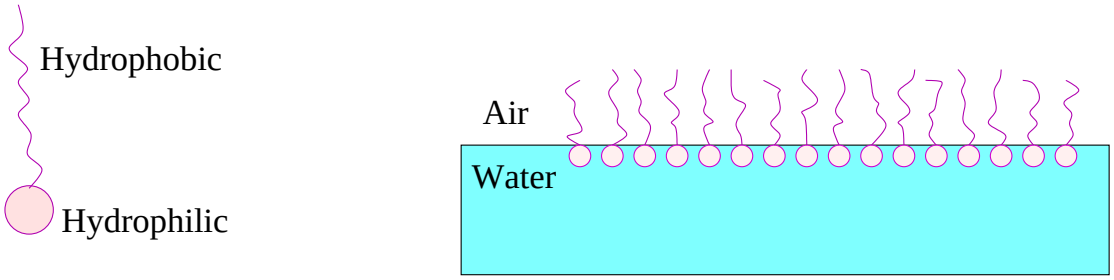

Figure 1.9: A schematic representation of amphiphilic molecules at the air-water interface.

of the molecules. Stable monolayers of the normal long-chain fatty alcohols or acids are formed if the chain length exceeds 12 carbon atoms. Since all the common naturally occurring fatty substances have even numbered chains (C_{14}, C_{16}, C_{18}, etc.), these derivatives have been extensively studied than their odd-numbered homologues. Amphiphiles are ubiquitous in biological systems. The lipids (e.g., phospholipids, cholesterol) are the basic constituents of the cell membrane and are amphiphilic in nature [9]. Some polymers including biopolymers are also known to exhibit amphiphilic character [10].

1.4.1 Discotic Mesogenic Amphiphiles

The discotic mesogenic molecules which exhibit amphiphilic character are known as discotic mesogenic amphiphiles. In the previous section, we have shown several discotic mesogens which consist of a π-conjugated rigid disk-shaped core surrounded by aliphatic chains. The core of these molecules are generally hydrophobic. However, appropriate polar groups (e.g., -OH, -COOH) can be attached with these disk-like cores via one or more aliphatic side chains. This introduces amphiphilic character in these molecules. On the surface of water, the discotic amphiphiles can exhibit two types of configuration; face-on and edge-on. In face-on configuration, the discotic core lies parallel to the water surface and the hydrocarbon tails extend away from the interface. Such a configuration may be preferred if the core of the molecule is capable of hydrogen bonding. In edge-on configuration, the discotic core lies normal to the water surface with the polar end submerged in water. Such a configuration leads to the formation of a two-dimensional analog of the columnar mesophase on the surface of water.

Apart from the synthetic discotic mesogenic amphiphiles, there are some naturally occurring biological disk-shaped molecules (e.g., vitamins, hemoglobin and chlorophyll) which are amphiphilic in nature (Figure 1.10).

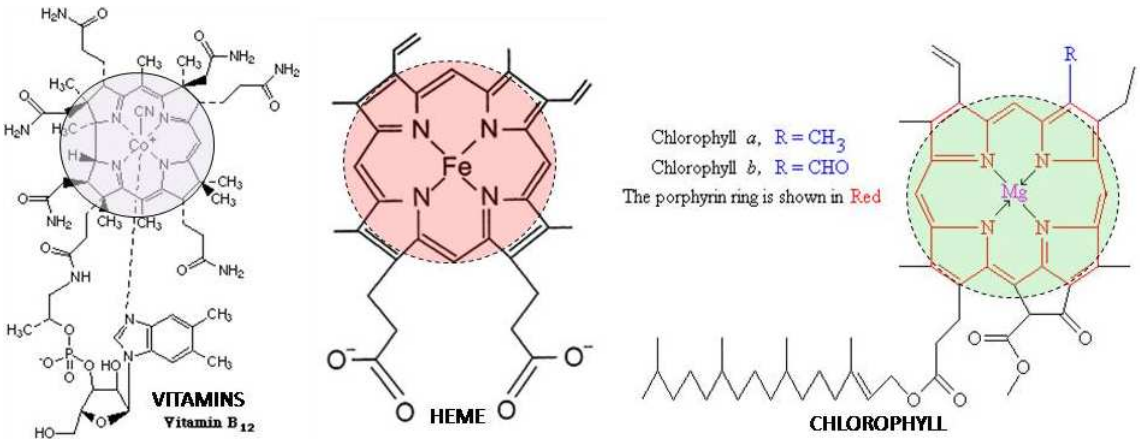

(a) (b) (c)

Figure 1.10: Examples of biologically important disk-shaped molecules.

1.5 Langmuir Monolayer

A mono-molecular layer of insoluble amphiphiles on the surface of an aqueous subphase is known as Langmuir monolayer [11]. To form a Langmuir monolayer, a dilute solution of such molecules dissolved in organic solvents (e.g., chloroform, methanol, benzene) is spread drop by drop on the surface of an aqueous subphase. The molecules spread spontaneously forming a monolayer on the surface of the subphase with its hydrophilic part immersed in the aqueous subphase and the hydrophobic part staying away from the aqueous subphase. The organic solvent used are volatile and evaporates in few minutes leaving back the amphiphilic molecules at the A-W interface. Consequently, the surface tension of water decreases. The difference between the surface tension of water without and with monolayer is called surface pressure. A Langmuir monolayer is an excellent model system for studying molecular ordering in two dimensions [12]. The aqueous subphase provides an ideally smooth surface. The surface pressure is varied simply by moving a barrier along the surface of the subphase, keeping the monolayer molecules on one side but letting the water flow freely below it. Such direct mechanical compression, a straightforward analog of hy-

drostatic compression in three dimensions, is not possible in any other two-dimensional system. Moreover, the intramonolayer and the monolayer-subphase interactions can be widely varied by changing the hydrophilic and hydrophobic parts of the molecules, or by changing the pH or ion content of the subphase [8].

Different types of interactions exist between the hydrophilic group and the subphase, amongst the hydrophilic groups and also amongst the hydrophobic groups [13]. The interactions that can exist between the hydrophilic (usually polar) groups can be ionic-ionic, dipole-dipole and ion-dipole. There can be van der Waals attractive interactions between the hydrophobic parts. Interactions between the hydrophilic group and the subphase is mainly governed by hydrogen bonding. Langmuir monolayer can decrease the rate of evaporation of subphase. The technique of Langmuir monolayer was commercialized for the first time to prevent evaporation in water reservoirs [14]. In addition, this technique is used to create model biological membranes to study structure and activity of lipids and proteins under controlled conditions [15].

As described in the previous section, there are wide varieties of amphiphilic molecules which are known to form stable monolayers on the surface of water. The most thoroughly investigated are various long-chain fatty molecules. Langmuir films of polymers, biological lipids (e.g., lung surfactant DPPC, cholesterol and its derivatives), and liquid crystals (e.g., biphenyl alkyl chains with cyano polar head group) are also well studied [10].

The first report on stable Langmuir monolayer formed by discotic amphiphiles dates back to 1985 [16]. Since then, there have been several reports on the formation of stable Langmuir monolayer of discotic mesogenic amphiphiles with a variety of disk-like cores and polar groups. Several disk-like biological molecules (e.g., vitamins, hemoglobin and chlorophyll) are also known to form stable Langmuir monolayers [17]. Although there have been studies on Langmuir monolayers of discotic amphiphiles with cores like triphenylene, phthalocyanines, truxene and hexacyclene [18] and polar groups like -OH and -COOH, there are no reports on ionic discotic mesogens at A-W interface. The ionic discotic mesogens are different from the conventional discotic mesogens. In this thesis, we have studied Langmuir monolayers of some novel ionic discotic mesogens based on triphenylene cores and explored some of their interesting properties.

1.6 Langmuir-Blodgett Film

A wealth of useful information about molecular ordering and intermolecular forces can be obtained from the studies of monolayers on the water surface. However, the great resurgence of interest in this area of science has been largely due to the fact that the monolayer films can be transferred from the water surface onto a solid substrate. Such films has become universally known as the Langmuir-Blodgett (LB) films [19]. The deposition is generally controlled by the stability of Langmuir monolayer and the hydrophilicity or hydrophobicity of the solid substrate on which the monolayer is transferred. The appealing features of LB films is the intrinsic control of the internal layer structure down to a molecular level and the precise control of the film thickness.

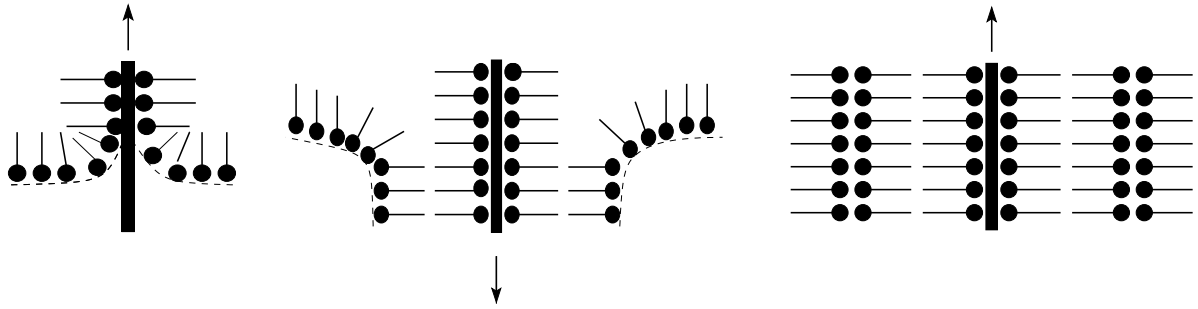

Figure 1.11: Conventional schematic of the LB technique using a hydrophilic substrate. To form the LB film, a substrate is passed through the air-water interface a given number of times, with each pass adding another monolayer to the LB film with alternating molecular orientations.

The process of building LB films consist of passing a solid substrate (e.g., glass, silicon wafers, quartz) alternately upwards and downwards through a Langmuir monolayer at the A-W interface [20]. A layer is deposited during each pass. The molecules deposited on the upward pass (upstroke) have their polar groups oriented towards the substrate while the molecules deposited on the down stroke are oriented with the hydrophobic groups facing the substrate. The result is that the polar groups adhere to the polar groups of the previous layer during the upstroke and the hydrophobic groups stick to the hydrophobic groups of the previous layer during the down stroke, in accordance with the expected behavior of amphiphilic molecules. The process is illustrated in Figure 1.11. There are several consequences of the dependence of molecular orientation upon dipping direction [21]. The initial layer can be deposited on the upstroke only on hydrophilic substrates since the hydrophobic tails will generally not adhere to such a substrate during a down stroke. Sim-

ilarly, the first layer will be deposited on the down stroke only on hydrophobic substrates. Moreover, the energetics of the amphiphilic interactions limit our ability to engineer required structures. Although monolayer transfer generally occurs during both upstroke and down stroke (Y-type deposition), under certain less common conditions, deposition can occur only during the down stroke (X-type) or the upstroke (Z-type).

During deposition of an individual LB layer, the surface area of the Langmuir monolayer on the water surface decreases due to the loss of molecules to the substrate. A simple diagnostic parameter of the deposition, the transfer ratio (τ), is defined as

$$\tau = \frac{Decrease\ in\ Langmuir\ monolayer\ \ surface\ area}{Total\ \ surface\ area\ of\ the\ substrate\ to\ be\ coated} \tag{1.1}$$

According to convention, a τ of unity is indicative of an ideal deposition. The acceptance of the value of unity as ideal, however, reflects an implicit assumption that the deposition process consists of simply transferring the molecules from the water surface to the substrate - creating a sort of replica. This assumption is often incorrect. LB transfer is a complicated process in which the amphiphiles generally attempt to reach a new thermodynamic minimum as they experience interactions with the solid substrate. If the molecular packing density changes during transfer, then $\tau = 1$ will not be the indicator of a defect-free film. However, in most of the fatty acid salt monolayers, the molecules on the water surface can be compressed into a nearly closed packed state before transfer and, although the details of the molecular packing may change, the molecules can remain densely packed after transfer. In such cases, the difference in packing density before and after will be a few percent at most, equivalent to the typical uncertainty of τ measurement.

Although various commercial applications have been proposed, ranging from anti reflection coating to soft X-ray monochromators, LB films have never truly found their way into the market place in a significant way. Nevertheless, the scientific interest in LB films remains strong after more than 70 years largely because the technique offers a controlled method for building supramolecular assemblies with well-defined molecular arrangement and orientation. LB films are extremely useful as a research tool in order to explore fundamental interactions of amphiphilic molecules, chemical reactions in confined geometries, and to create model biological systems. From a statistical physics standpoint, LB films offer the possibility of studying the evolution of structure and

phase transitions as a system evolves from two to three dimensions [22].

1.7 Experimental Techniques

There are several techniques to study the monolayer films at the A-W and air-solid (A-S) interfaces. We have used surface manometry, Brewster angle microscopy and reflection microscopy to study the films at the A-W interface. For studying the films at A-S interface, we have used various modes of a scanning probe microscope. In this section, we briefly describe these techniques.

1.7.1 Surface Manometry

Surface manometry is a standard method to study the phase transition in Langmuir monolayers. Here, the surface pressure (π) is varied as a function of the area per molecule (A_m) at constant temperature. The A_m is the inverse of surface density. The π is given by the difference in the surface tension of water without monolayer and with monolayer. The surface density of the molecules can be varied by compression of the monolayer using barriers. Figure 1.12 shows the schematic diagram of a Langmuir trough.

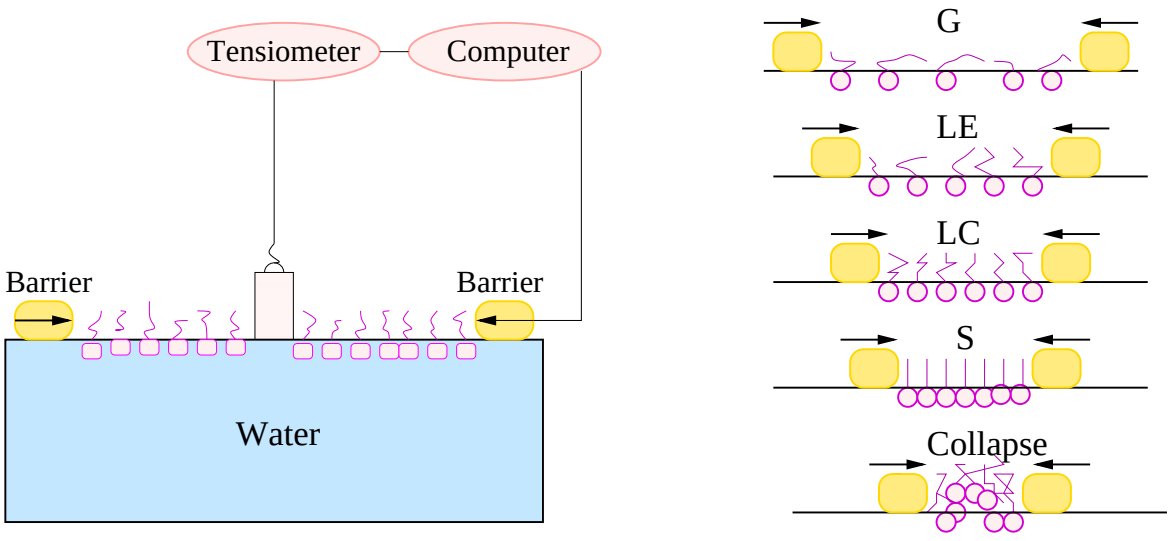

Figure 1.12: A schematic diagram of the Langmuir trough showing the experimental setup for the measurement of surface pressure (π) - area per molecule (A_m) isotherm. The molecular arrangement in different phases are shown on the right. The symbols G, LE, LC and S represent gas, liquid expanded, liquid condensed and solid phases, respectively.

The set up consists of a teflon trough with barriers which are driven by a DC motor interfaced to a computer. The trough is kept on a granite slab to damp the vibrations. In the experiments, the trough was cleaned with utmost care since traces of impurities reduce the surface tension. The trough was filled with Millipore Milli-Q water of high purity (specific resistance was greater than 18.2 MΩ-cm) for carrying out the surface manometry studies. The Wilhelmy plate method was used to measure the surface pressure. Here, a filter paper of dimension 1 cm width and 2 cm length was used as a Wilhelmy plate. It was suspended from a sensor head using a hook. The filter paper was immersed into the subphase and allowed to equilibrate. The principle of Wilhelmy plate method lies in measuring the vertical component of the force due to surface tension. The surface pressure π is given by

$$\pi = \gamma_0 - \gamma \tag{1.2}$$

where γ_0 is the surface tension of pure water ($\sim$ 72 mN/m at 23^0C), γ is the surface tension of water with monolayer. The sensor generates an electric signal proportional to the force acting on the filter paper which was calibrated with known weights. The sensitivity of the sensor was 0.1 mN/m. The material was dissolved in chloroform. The usual concentration was around 0.2 mg/ml. The solution was spread on the surface of ultra pure water using a Hamilton micro syringe. About 15 minutes were allowed for the solvent to evaporate. The A_m was varied by compressing the barrier and the corresponding surface pressure was measured.

A typical π - A_m isotherm is shown in Figure 1.13. Here, the monolayer phase starts from gas (G), followed by G + liquid expanded (LE), LE + liquid condensed (LC), LC, solid (S) and finally collapses into three dimensional structures. At very large A_m, the monolayer is predominantly in the G phase. In this phase, the molecules are far apart and they have no interactions. At lower A_m, there is an increase in the surface pressure indicating a phase transition to LE phase. In this phase the chains and the polar heads come closer and are randomly arranged. At still lower A_m, the LE phase transforms to LC phase and finally to S phase. In LC phase, the chains have tilt and there is a quasi-long range order in the polar heads. In S phase, the molecules are compactly packed and the chains are untilted. Further compression leads to the collapse of the monolayer where it

transforms to crystallites or multilayers. The coexistence of phases between the transformations appears as plateau region in the isotherm.

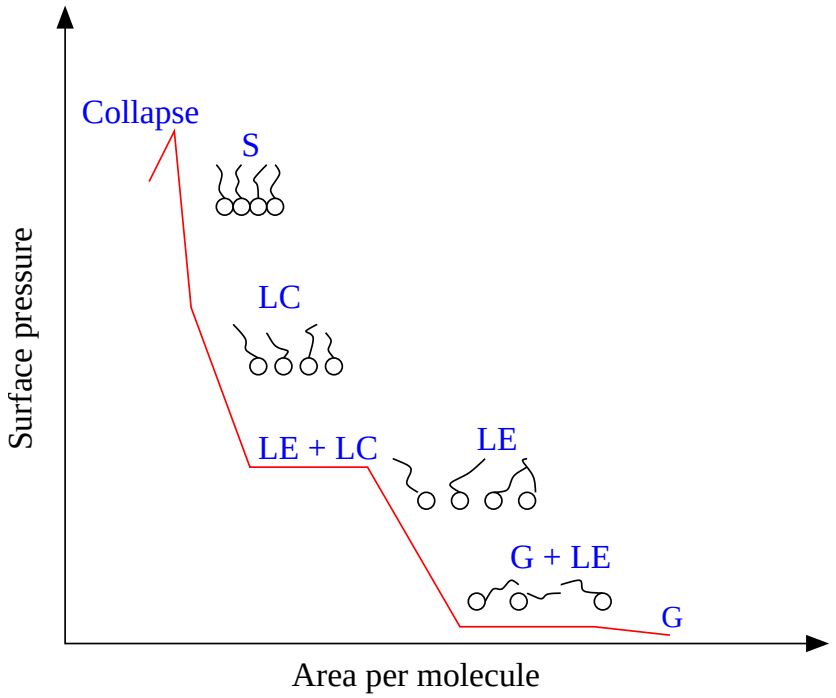

Figure 1.13: A typical isotherm indicating the different phases in a Langmuir monolayer. The symbols G, LE, LC and S represent gas, liquid expanded, liquid condensed and solid phases, respectively. The kink in the isotherm is associated with a phase transition.

Prior to performing the π - A_m isotherm measurements, one can test the spreading capability of molecules at the A-W interface by measuring the equilibrium spreading pressure (ESP). This is the surface pressure at which the monolayer coexists with its bulk phase at the A-W interface [8]. When a speck of crystallite is placed on the water surface, the molecules from the bulk crystallites elude out and form a monolayer at the interface spontaneously. After a certain period of time, the system reaches an equilibrium state where the rate of elution of molecules from crystallites is equal to the rate of molecules binding to the crystallites. The variation in surface pressure with time shows an initial increase in surface pressure due to the formation of monolayer. On reaching the equilibrium, the surface pressure value saturates. The saturated value of surface pressure is known as ESP. The finite value of ESP can suggest the monolayer to be stable against dissolution or evaporation of the molecules. The ESP values of some molecules like stearic acid, octadecanol and dipalmitoyl phosphatidylcholine are 5.2, 34.3 and 1 mN/m, respectively [23].

We have used a commercial Langmuir trough (model: 611M, NIMA Technology, Coventry, England) for all our surface manometry experiments. The trough was equipped with a motor controlled vertical dipper for the LB film deposition.

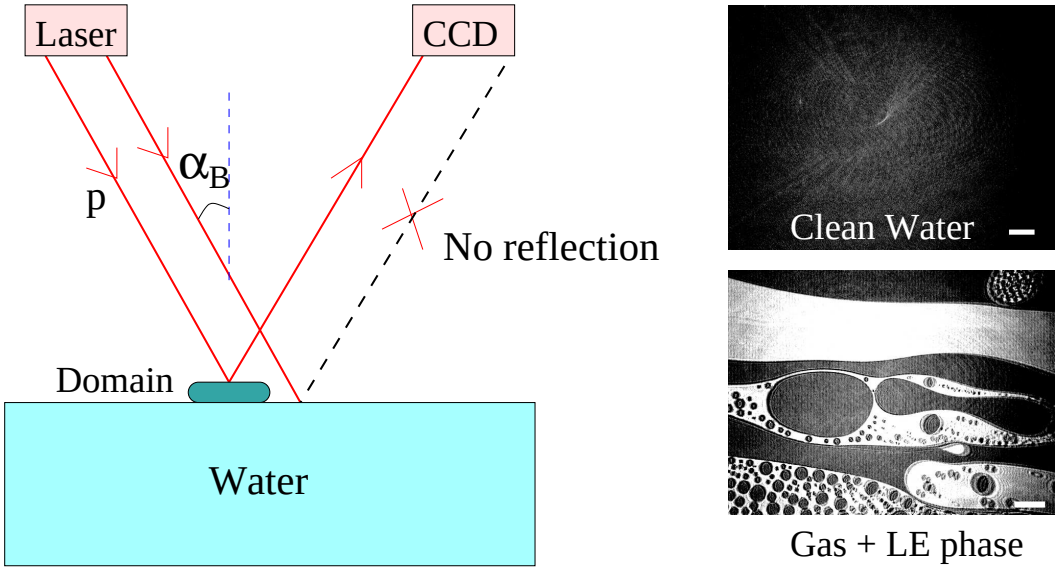

Figure 1.14: A schematic diagram showing the working principle of a Brewster angle microscope. α_B is the Brewster angle of water with respect to air.

1.7.2 Brewster Angle Microscopy

Brewster angle microscope (BAM) was developed by Henon et al. [24] which is now been widely used for studying the morphology of films, both on liquid and on solid surfaces [25]. The working principle of a Brewster angle microscope is shown in Figure 1.14. At an interface, where the refractive index changes, the reflectivity of the in-plane polarization (p-polarized) component becomes almost zero at the Brewster angle. The Brewster angle α_B is given by

$$tan\,\alpha_B = \frac{n_{water}}{n_{air}} \tag{1.3}$$

where n_{water} and n_{air} are the refractive indices of water and air, respectively. When the p-polarized laser beam is incident on the water surface at Brewster angle (53.1°), the reflection from the water surface is negligible. When the monolayer is spread, the Brewster angle condition is no

longer satisfied. The monolayer domain, having a different index of refraction, will cause a small amount of light to be reflected. This is typically of the order of 10^{-6} of the incident light but still enough to form an image with a CCD camera. The reflectivity at the interface is dependent on the thickness, roughness and anisotropy of monolayers. Domains with different orientation or tilt give rise to different contrasts. We have used a commercial setup, miniBAM (Nanofilm Technologie GmbH, Germany) with a laser of 30 mW at 660 nm wavelength for all our BAM studies.

1.7.3 Reflection Microscopy

Multilayers which are sufficiently thick (of the order of 1 μm) could be observed under reflection microscope. Light striking normally on the thicker domains get interfered from the air-domain interface and domain-water interface leading to interference colors. The minimum thickness d of the film can be calculated using,

$$d = \frac{\lambda}{2\eta} \tag{1.4}$$

where λ is the wavelength of light in the visible region and η is the effective refractive index of the film. The minimum thickness which can be resolved is around 0.2 μm (taking η = 1.5 and λ = 500 nm). Using this technique, one can interpret the shape of the domains. If the interference color is uniform it indicates a flat domain. A pattern with concentric rings indicates a lens shaped domain. We have used a Leitz Metalux 3 microscope for our reflection microscopy studies.

1.7.4 Scanning Probe Microscopy

In a scanning probe microscope (SPM), an image is created by scanning with a sharp tip over a sample surface and measuring some highly localized tip-sample interaction as a function of position. The major types of SPM include scanning tunneling microscope (STM), which measures tunneling current, and atomic force microscope (AFM), which measures force interactions. The first instrument capable of directly obtaining three-dimensional images of solid surfaces with atomic resolution is the STM developed by Binnig and his colleagues in 1981 at the IBM Zurich

Research Laboratory, Switzerland [26]. However, STM can only be used to study surfaces which are electrically conductive. Based on their design of the STM, in 1985, Binnig et al. developed AFM to measure ultrasmall forces (less than 1μN) present between the AFM tip and the sample surface [27]. AFM does not require a substrate to be electrically conductive as in the case of STM. AFM can image all types of surfaces irrespective of their electrical, mechanical and optical properties. This has made AFM the most widely used form of SPM. We have used a commercial scanning probe microscope (model: PicoPlus, Molecular Imaging, USA) for all our AFM studies.

The operation of AFM relies on the forces between the tip and sample. AFM tips and cantilevers are microfabricated from silicon or silicon nitride. Typical tip radius is from a few to tens of nm. The force is not measured directly, but calculated by measuring the deflection of the cantilever, and knowing the stiffness of the cantilever. Hook's law gives $F = -k_c z$, where F is the force, k_c is the stiffness of the cantilever, and z is the cantilever deflection. To detect cantilever deflection, an optical beam deflection method is commonly used where a laser beam is reflected from the back of the cantilever onto a split photodiode detector. The sub-angstrom deflections can be detected and, therefore, force down to picoNewton is measured. A more recently developed method of cantilever deflection measurement is through a piezoelectric layer on the cantilever that registers a voltage upon deflection [28].

In an AFM, when the tip approaches the sample surface, it experiences various interaction forces. Figure 1.15 shows a typical force versus tip-sample distance curve as the tip approaches the sample surface. When the tip is far from the sample (more than 10 μm), the tip is free from any interaction and no deflection of the cantilever is detected. The first interaction encountered by the tip as it approaches the sample is due to the damping air film. This is developed when an oscillating tip comes to within 10 μm of the sample surface. At this distance, air is squeezed between the tip and the surface during each down stroke of the tip. This pumping effect dampens the tip motion to some extent. The air film damping phenomenon is exclusive to oscillating cantilevers; contact mode AFM and STM tips do not produce the phenomenon. As the tip approaches the sample in the range of 1 to 0.1 μm, electrostatic forces are encountered. Electrostatic forces may be either

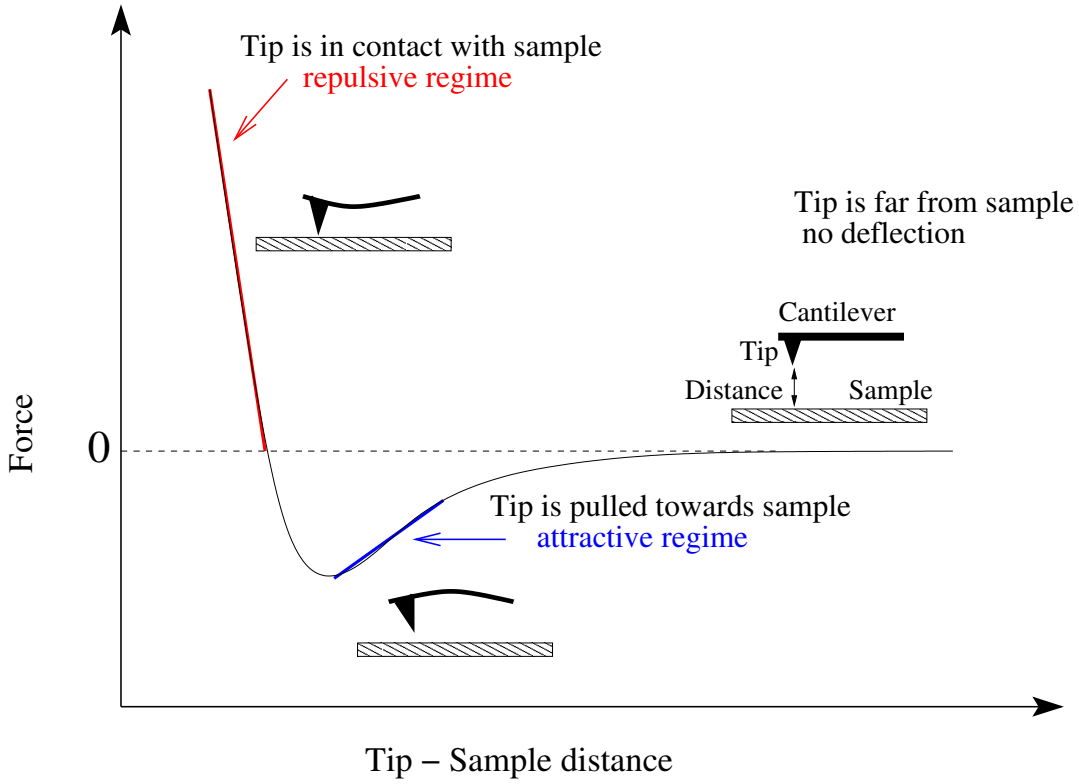

Figure 1.15: The schematic representation of a typical force versus tip-sample distance curve in an atomic force microscope.

attractive or repulsive and vary according to the material. At a distance of 200 to 10 nm above the sample surface, the tip experiences the surface tension effects. This effect results from the presence of condensed water vapor at the sample surface. This is an attractive force, and can pull a tip down towards the sample surface and strong enough to indent very soft materials. Usually, oscillating cantilevers are employed to overcome the effects of surface tension. If delicate samples are to be imaged, it may be necessary to immerse both tip and sample entirely in a liquid to prevent surface tension attraction. When the tip further approaches at the angstrom level above the surface, van der Waals forces cause a weak attraction between atoms in the tip and sample. When the tip reaches sub-angstrom level above the surface, it experiences coulombic repulsion force and the tip - sample are said to be in 'contact'. At this level, electron shells from atoms on both tip and sample repulse one another, preventing further intrusion into each other. Force exerted beyond this level leads to mechanical distortion of one or both materials, and the tip may be damaged [29].

Since AFM can measure variety of forces, including van der Waals forces, electrostatic forces, magnetic forces, adhesion forces and frictional forces, specialized modes of AFM are developed to characterize the electrical [30], mechanical [31] and chemical [32] properties of a sample in addition to its topography.

1.7.4.1 Contact Mode AFM

This is the basic mode of operation in which a piezoelectric scanner rasters the tip over the sample surface. The forces between the tip and sample are measured through deflections of the cantilever. A feedback loop monitors the tip-sample force and adjusts the tip vertical position (Z-position) to hold the force constant. Therefore, a constant height is maintained above the surface. The topographic image of the sample is constructed from the tip Z-position data. A schematic representation of AFM operation in contact mode is shown in Figure 1.16. This mode is called contact mode because the tip is deflected by the sample due to repulsive forces, or 'contact'. As the tip is in contact with the surface, the stiffness of the cantilever needs to be less than that of the effective spring constant holding atoms together, which is of the order of 1-10 nN/nm. Most contact mode cantilevers have a spring constant of < 1 N/m. It is generally used for flat samples that can withstand lateral forces during scanning.

Moreover, the lateral forces can measure the friction between the tip and the sample surface [33]. As the sample is scanned back and forth in a direction orthogonal to the long axis of the cantilever beam, the friction force between the tip and the sample produces a twisting of the cantilever. Consequently, the laser beam gets reflected out of the plane defined by the incident beam and the beam reflected vertically from an untwisted cantilever. This produces an intensity difference of the laser beam received in the left hand and right hand sets of quadrants of the photo detector (Figure 1.16, lateral deflection ((A+C)-(B+D))). The intensity difference between the two sets of detectors is directly related to the degree of twisting and hence to the magnitude of the friction force.

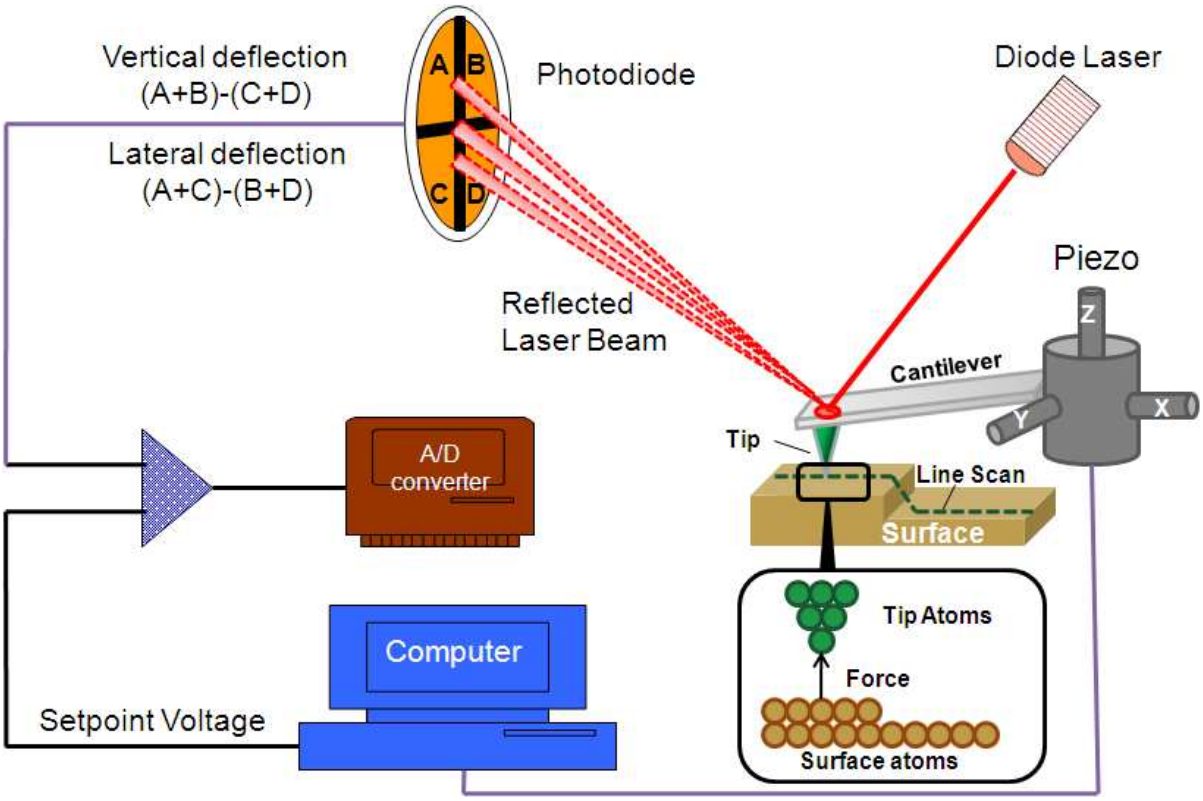

Figure 1.16: A schematic diagram showing the working principle of an atomic force microscope in the contact mode.

1.7.4.2 AC Mode AFM

The lateral shear forces in the contact mode cause damage to very soft samples like biological membranes. To minimize this damage, AC mode has been developed [34]. In this mode, the cantilever is driven into AC oscillation near its resonant frequency with a constant amplitude. When the tip approaches the sample, the oscillation is damped, and the reduced amplitude is the feedback signal. The topography image is constructed from the varying Z-position of the tip required to keep the tip oscillation amplitude constant. In addition, the phase shift of the oscillating cantilever relative to the driving signal is measured. This phase shift can be correlated with specific material properties that affect the tip-sample interaction. The phase shift can be used to differentiate areas on a sample surface with different properties such as stiffness, adhesion, and viscoelasticity. A schematic representation of AFM operation in AC mode is shown in Figure 1.17.

On the basis of the tip-sample interaction regime, the AC mode AFM can be classified into two modes of operation: Intermittent contact mode and non-contact mode. The schematic illustration

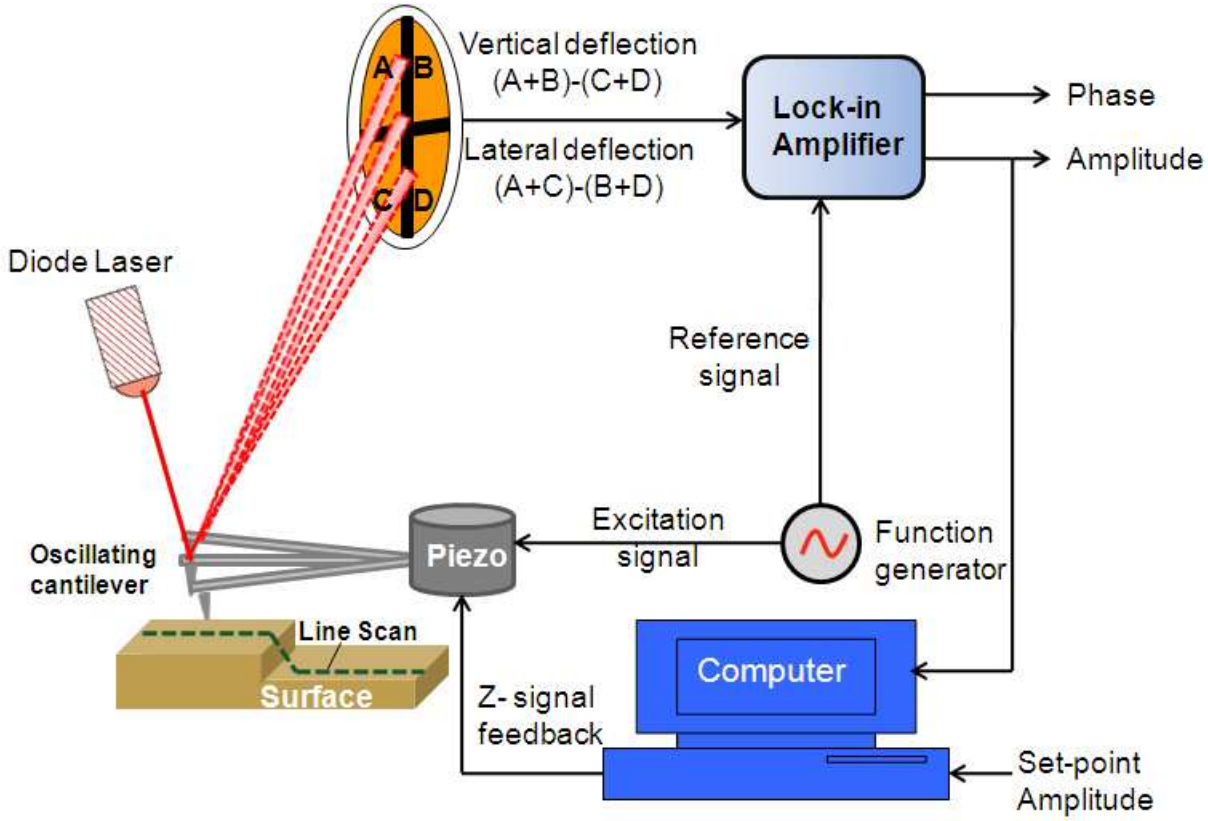

Figure 1.17: A schematic diagram showing the working principle of an atomic force microscope in the AC mode.

of the distance-dependent regimes of interaction between an oscillating cantilever and a sample surface is shown in Figure 1.18. In intermittent contact mode (also called tapping mode), the tip contacts the sample in each cycle for a small duration ($\sim 10^{-7}$ seconds). Therefore, the amplitude is reduced by the repulsive interaction as in the contact mode. In non-contact mode, long-range van der Waals forces which are attractive in nature, reduce the amplitude of oscillation.

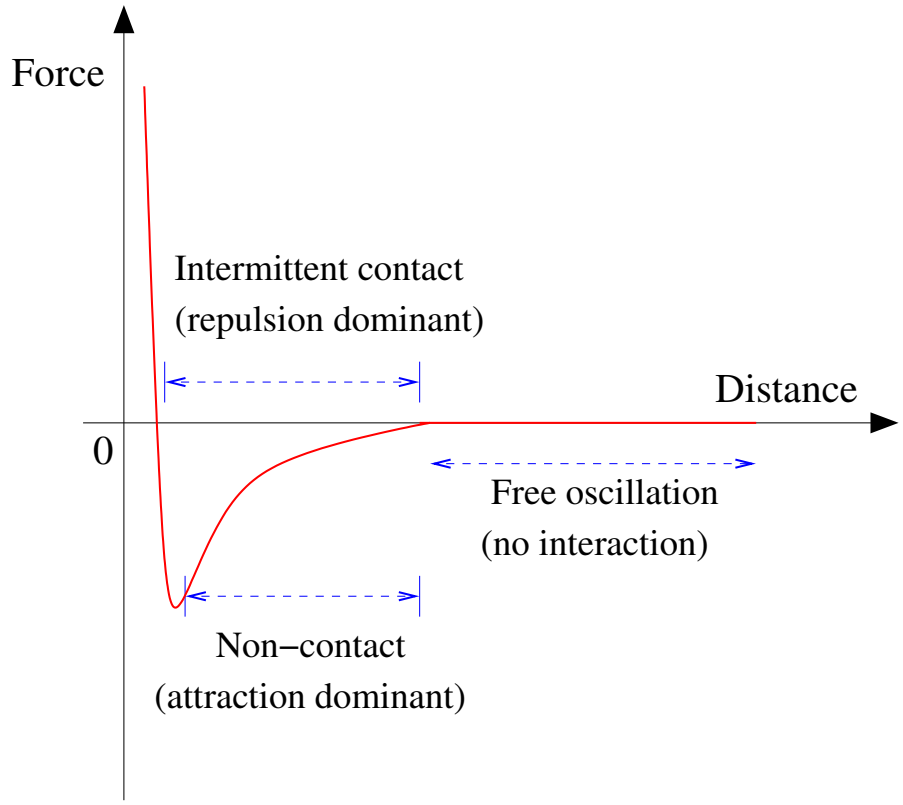

Figure 1.18: Schematic illustration of the distance-dependent regimes of interaction between an oscillating cantilever and a sample surface. Dashed horizontal line segments denote distance intervals explored by the tip in each regime. The interaction regimes are labeled as free oscillation (no interaction), non-contact (attraction dominant), and intermittent contact (repulsion dominant).

1.7.4.3 Current-Sensing AFM

Current-sensing atomic force microscopy (CS-AFM) is a powerful technique for characterizing conductivity variations on a sample surface. It allows current measurements in the range from picoAmperes to microAmperes. Here, the AFM tip is made conducting by coating the silicon nitride or silicon tips with metals like gold or platinum. The technique of CS-AFM is essentially a two-probe measurement, with the conducting tip of AFM as one electrode and the conducting substrate

as the other electrode. Usually, this technique works in the conventional contact mode AFM [35]. With the tip at virtual ground, a selectable bias voltage is applied to the conducting substrate . By maintaining a constant force between the tip and sample, simultaneous topographic and current images are generated. This enables a direct correlation of local topography with electrical properties. In addition, we can measure current-voltage characteristics by placing the tip at a desired position on the sample under controlled load. This can give valuable information about the electron transport mechanism at the tip-sample interface. Figure 1.19 shows a schematic representation of the working principle of a CS-AFM.

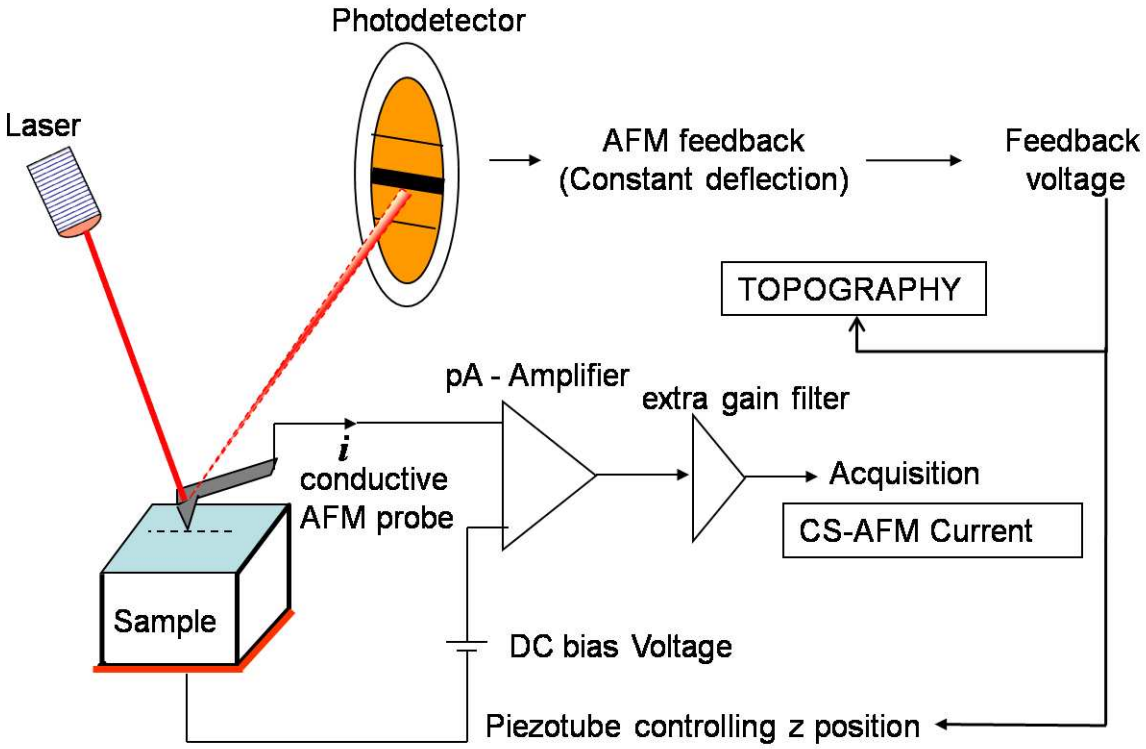

Figure 1.19: A schematic diagram showing the working principle of a current-sensing atomic force microscope.

A scanning tunneling microscope (STM) which works on the principle of tunneling current between the tip and sample, can also be used to study the electrical conductivity of samples. Unlike CS-AFM, in STM the probe is positioned using tunneling current as the feedback parameter. It becomes difficult to decouple the probe positioning from the sample conductivity. Hence, the surface topography of the film and its electrical conductivity can not be acquired independently.

In addition, there is a tunnel gap of about 0.3 to 1 nm between the STM tip and the sample surface. Therefore, the actual distance between the STM tip and the sample surface is not known. This makes the quantitative analysis of the current-voltage characteristics obtained in STM measurements difficult, whereas, such analysis is straightforward in CS-AFM measurements due to the absence of any tunnel gap. In CS-AFM, the distance between the tip and the substrate can be taken as the sample thickness itself since the tip is in contact with the sample. Figure 1.20 shows schematically the basic difference in conductance measurements using a STM and a CS-AFM.

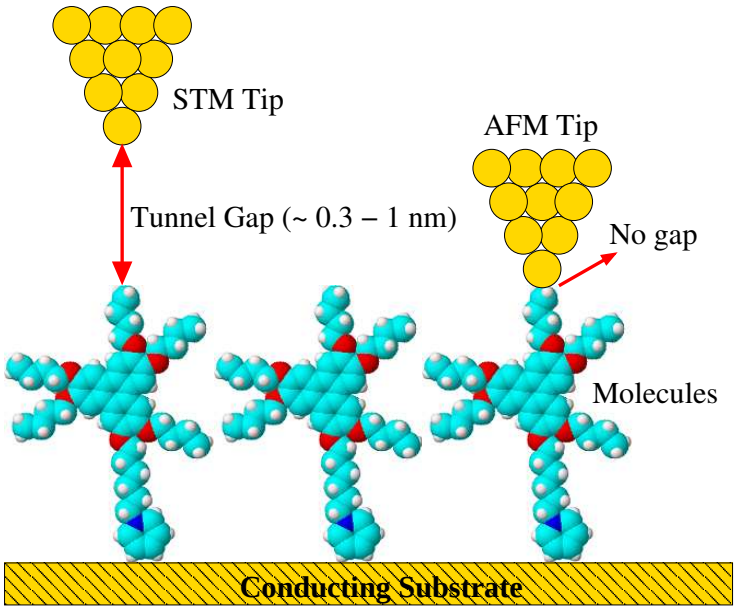

Figure 1.20: Schematic diagram showing the basic difference in conductance measurements using a STM and a current-sensing AFM.

Thus, AFM has become a popular scanning probe technique. The electrical properties like conductivity and mechanical properties like hardness, elasticity and stiffness can be measured with nanometer scale resolution using an AFM. The greatest advantage is that it can be used for any material and in any environment such as ambient air, various gases, liquid and vacuum [36].

Bibliography

[1] P. G. De Gennes and J. Prost, *The Physics of Liquid Crystals*, Oxford University Press: UK, (2001).

[2] P. J. Collings and M. Hird, *Introduction to Liquid Crystals: Chemistry and Physics*, Taylor and Francis: London, (1997).

[3] W. M. Gelbart, A. Ben-Shaul, and D. Roux, *Micelles, membranes, micro-emulsions, and monolayers*, Springer-Verlag: New York, (1994).

[4] Sandeep Kumar, *Chem. Soc. Rev.* **35**, 83 (2006).

[5] S. Chandrasekhar, B. K. Sadashiva, and K. A. Suresh, *Pramana* **9**, 471 (1977).

[6] S. Sergeyev, W. Pisula, and Y. H. Geerts, *Chem. Soc. Rev.* **36**, 1902 (2007).

[7] Sandeep Kumar and S. K. Varshney, *Angew. Chem. Int. Ed.* **39**, 3140 (2000).

[8] G. L. Gaines Jr., *Insoluble Monolayers at Liquid Gas Interface*, Interscience: New York, (1966).

[9] M. L. Longo, A. M. Bisagno, J. A. N. Zasadzinski, R. Bruni, and A. J. Waring, *Science* **261**, 453 (1993).

[10] K. S. Birdi, *Lipid and Biopolymer Monolayers at Liquid Interfaces*, Plenum: New York, (1989).

[11] I. Langmuir, *J. Am. Chem. Soc.* **39**, 1848 (1917).

[12] V. M. Kaganer, H. Mohwald, and P. Dutta, *Rev. Mod. Phys.* **71**, 779 (1999).

[13] J. N. Israelachvili, *Intermolecular and Surface Forces*, Academic Press: London, 1992.

[14] P. W. Sylvia, *New Scientists* **24**, 1 Nov. 2003.

[15] I. Langmuir and V. J. Schaefer, *J. Am. Chem. Soc.* **60**, 1351 (1938).

[16] D. W. Kalina and S. W. Crane, *Thin Solid Films* **134**, 109 (1985).

[17] I. Langmuir and V. J. Schaefer, *J. Am. Chem. Soc.* **59**, 2075 (1937).

[18] N. C. Maliszewskyj, P. A. Heiney, J. K. Blasie, J. P. McCauley, and A. B. Smith *J. Phys. II France* **2**, 75 (1992).

[19] D. K. Schwartz, *Surf. Sci. Rep.* **27**, 241 (1997).

[20] K. B. Blodgett, *J. Am. Chem. Soc.* **57**, 1007 (1935).

[21] G. Roberts, *Langmuir-Blodgett Films*, Plenum Press: New York, 1990.

[22] D. H. McCullough III and S. L. Regen, *Chem. Commun.*, 2787 (2004).

[23] R. D. Smith and J. C. Berg, *J. Colloid Interface Sci.* **74**, 273 (1980).

[24] S. Henon and J. Meunier, *Rev. Sci. Instrum.* **62**, 936 (1991).

[25] G. A. Overbeck, D. Honig, and D. Mobius, *Langmuir* **9**, 555 (1993).

[26] G. Binnig, H. Rohrer, Ch. Gerber, and E. Weibel, *Phys. Rev. Lett.* **49**, 57 (1982).

[27] G. Binnig, C. F. Quate, and Ch. Gerber, *Phys. Rev. Lett.* **56**, 930 (1986).

[28] R. Linnemann, T. Gotszalk, I. W. Rangelow, P. Dumania, and E. Oesterschulze, *J. Vac. Sci. Technol. B* **14**(2), 856 (1996).

[29] B. Cappella and G. Dietler, *Surface Science Reports* **34**, 1 (1999).

[30] C. Ionescu-Zanetti, A. Mechler, S. A. Carter, and R. lal, *Adv. Mater.* **16**, 385 (2004).

[31] E. W. Wong, P. E. Sheehan, and C. M. Lieber, *Science* **277**, 1971 (1997).

[32] Y. Sugimoto, P. Pou, M. Abe, P. Jelinek, R. Perez, S. Morita, and O. Custance *Nature* **446**, 64 (2007).

[33] B. Bhushan, J. N. Israelachvili, and U. Landman, *Nature* **374**, 607 (1995).

[34] F. J. Giessibl, *Phys. Rev. B* **56**, 16010 (1997).

[35] D. J. Wold and C. D. Frisbie, *J. Am. Chem. Soc.* **122**, 2970 (2000).

[36] F. J. Giessibl, *Rev. Mod. Phys.* **75**, 949 (2003).